AIP | The Journal of Chemical Physics

Electron impact ionization and multiphoton ionization of doped superfluid helium droplets: A comparison

Yunteng He, Jie Zhang, and Wei Kong

Citation: The Journal of Chemical Physics **144**, 084302 (2016); doi: 10.1063/1.4942473
View online: http://dx.doi.org/10.1063/1.4942473
View Table of Contents: http://scitation.aip.org/content/aip/journal/jcp/144/8?ver=pdfcov
Published by the AIP Publishing

Electron impact ionization and multiphoton ionization of doped superfluid helium droplets: A comparison

Yunteng He, Jie Zhang, and Wei Kong[a)]
Department of Chemistry, Oregon State University, Corvallis, Oregon 97331, USA

(Received 25 December 2015; accepted 8 February 2016; published online 24 February 2016)

We compare characteristics of electron impact ionization (EI) and multiphoton ionization (MPI) of doped superfluid helium droplets using the same droplet source. Selected dopant ion fragments from the two ionization schemes demonstrate different dependence on the doping pressure, which could be attributed to the different ionization mechanisms. While EI directly ionizes helium atoms in a droplet therefore has higher yields for bigger droplets (within a limited size range), MPI is insensitive to the helium in a droplet and is only dependent on the number of dopant molecules. The optimal timing of the ionization pulse also varies with the doping pressure, implying a velocity slip among different sized droplets. Calculations of the doping statistics and ionization probabilities qualitatively agree with the experimental data. Our results offer a word of caution in interpreting the pressure and timing dependence of superfluid helium droplets, and we also devise a scheme in achieving a high degree of doping while limiting the contribution of dopant clusters. © *2016 AIP Publishing LLC.* [http://dx.doi.org/10.1063/1.4942473]

INTRODUCTION

Superfluid helium droplets have proven to be a versatile medium to isolate and cool both neutral and ionic species for spectroscopic and other fundamental studies, and for generation of esoteric species.[1–4] Recently, our group has introduced electron diffraction of doped superfluid helium droplets for single molecule diffraction[5] with the ultimate goal of structure determination from Fraunhofer diffraction of oriented molecules.[6] Among the many research activities involving superfluid helium droplets, ionization of pure and doped helium droplets has been intensively studied.[7–10] In fact, mass spectrometers have played and continue to play a crucial role in the development of techniques involving superfluid helium droplets. As the most inert element, helium has the highest ionization potential, hence electron impact ionization (EI) has been the initial choice.[10,11] Upon collision with sufficiently high energy electrons, He_n^+ ($n \geq 1$) has been observed and the presence of these cluster ions has been regarded as evidence of helium droplets. If neutral dopant molecules are present in the droplet, bare fragment ions of dopant and cluster ions of dopant fragments with helium atoms and helium clusters have also been observed.[12,13] A prevailing theory on the mechanism of electron impact ionization is the charge hopping model,[14,15] where the first target of ionization is a helium atom on a droplet. Then He^+ undergoes resonant hopping inside the droplet until the charge localizes or until it encounters a dopant molecule. The ionization yield of electron impact ionization therefore decreases with decreasing droplet size.

Photoionization of doped helium droplets has been investigated using synchrotron sources, femtosecond lasers, and nanosecond pulsed lasers.[7] In the extreme ultraviolet region where the photon energy is above the ionization threshold of helium, direct ionization of both helium and dopant molecules is possible.[16,17] However, given the presence of thousands to millions of helium atoms compared with one neutral molecule, direct ionization of helium probably dominates the first ionization event. For light sources with lower photon energies, multiphoton ionization (MPI) is typically required.[18–20] Since ionization of a ground state helium atom requires more photons than that of a neutral dopant molecule, in MPI, dopant molecules are the frontline species of direct ionization. Hence depending on the experimental procedure, different modes of photoionization occur with different fragmentation patterns even for the same doped species.[7,21]

In all previous literature reports, typically only one type of ionization processes was employed in one laboratory.[7,9,13] Our group has employed both electron impact ionization and multiphoton ionization mass spectrometry in the same vacuum system,[20] which enables us to directly compare the yields and sensitivities of the two types of processes. We measure the ionization fragments under different droplet source conditions and different doping conditions, with two essentially exchangeable dopant molecules, CCl_4 and CBr_4. Our results are surprising at first sight, and we attribute the difference between EI and MPI to the different ionization mechanisms. We also offer a word of advice in choosing a diagnostic tool for the performance of a neutral doped helium droplet beam, particularly for pulsed beams, and we also devise a condition to maximize the fraction of doped droplets while still limiting the formation of dopant clusters.

EXPERIMENTAL SETUP

A schematic of our experimental arrangement has been described in our previous publication.[20] The pulsed droplet beam was formed by supersonic expansion of helium (Airgas,

a)Author to whom correspondence should be addressed. Electronic mail: wei.kong@oregonstate.edu. Tel.: 541-737-6714.

99.9995%) from an Even-Lavie pulsed valve with an electric driving pulse of 24.8 μs in duration. The droplet beam passed a 2 mm dia. skimmer to enter the pickup chamber and a 5 mm dia. home-made conical cone to enter the main chamber. The pressure of the doping chamber was measured by an ionization gauge located ~12 cm away from the droplet beam. Two home-made time-of-flight (TOF) mass spectrometers were used in the main chamber: one in-line with the droplet beam (EI-TOF) and the other (MPI-TOF) perpendicular to the beam. The overall system ran at 5 Hz, and in between droplet pulses, a background spectrum was taken as the reference, so the repetition rate of the ionization pulse, either electrons or photons from a laser, was 10 Hz. The difference between the signals from the doped droplets and the background should therefore be the representative of the net effect of the droplet beam, independent of any slow drifts in the experimental condition. This aspect was crucial particularly when doping with a gaseous sample such as CCl_4, and the doping gas could diffuse into the main chamber and contribute to the background.

For the EI-TOF, the ionization source was a heated tungsten filament, and the electrons were momentarily energized by a pulsed grid to 300 V for ionization. The ionization pulse of 4 μs was superimposed on a constant offset of −70 V on the extraction electrode, and the falling edge of the ionization pulse was the starting time of the time-of-flight mass spectrum. The ionization potentials for CCl_4 and CBr_4 are 11.5 eV[22] and 10.3 eV,[23] respectively, and intense fragmentation is expected in the mass spectrum. Limited by the not-well-defined ionization region of the electron source and the initial velocity of the droplets, the mass resolution of the EI-TOF was insufficient to resolve small fragments of dopant molecules from cluster ions of helium. However, when doping with CCl_4, the signal from CCl_3^+ was sufficiently shifted from the congested region where helium cluster ions He_n^+ are significant. Consequently, CCl_3^+ was chosen as the signature of the doped droplet.

We used the 4th harmonic of a nanosecond Nd:YAG laser (Quantel, Brilliant) for non-resonant multiphoton ionization. With a power density of 10^{10} W/cm^2 at 266 nm, only dopant molecules could be ionized. The mass spectrometer was similarly designed as the EI-TOF,[20] except that the flight tube was less than 1/3 of the length of the EI-TOF, and it was perpendicular to the traveling direction of the droplet beam. Nevertheless, the well defined ionization region and time from the focused laser resulted in high resolution mass spectra, and fragments of dopant molecules and clusters of dopant fragments with helium atoms, including $(He)_nC^+$, $(He)_nCl^+$, and $(He)_nCCl^+$ (n = 0–9), were observable. Unfortunately, easy fragmentation in the presence of a photon flux at 10^{28} photons/s cm^2 severely limited the yield of the larger CCl_3^+ ions. Attempts to lower the intensity of the laser beam by reducing the laser power and by shifting the focal point of the laser did not yield any substantial difference in the fragmentation pattern. Given the complexity of the ionization mechanism, no further effort was dedicated to further decipher the fragmentation pattern. The largest detectable dopant fragment was CCl^+ and its complexes with helium, and the intensity of bare CCl^+ was about 1/3 less than that of Cl^+. Consequently, here we use the intensity of the light fragment Cl^+ as a signature of the doped droplet.

RESULTS

Dependence of ionization yield on doping pressure

The traces labeled "fixed timing" in Figure 1 show the dependence of signature fragments from EI and MPI on the doping pressure. The stagnation pressure and temperature of the pulsed valve were kept at 50 atm and 16 K. The presence of CCl_3^+ from the EI-TOF is only observable within a small pressure range, and the maximum signal corresponds to a doping pressure of 6×10^{-6} Torr. The timing of the ionization pulse was therefore set based on the signal at 6×10^{-6} Torr and so was the normalization of the ion yields under different doping pressures. The profile of Cl^+ from MPI is normalized to be comparable with that from the EI-TOF, but the actual signal intensity from the MPI experiment was more than 3 orders of magnitude larger than that from the EI-TOF. The timing of the ionization laser was set based on the optimal signal at 1×10^{-5} Torr.

The results in Fig. 1 are surprising at first sight—they reveal different optimal doping conditions for the two different experiments. Signal from the MPI-TOF reaches its peak after that from the EI-TOF has dropped to a negligible level. Although the spectrometers are not identical, and limited by the resolution and mass range, different fragments are used in Fig. 1, the different responses of the two spectrometers to the doping pressure of the same droplet beam are still unexpected.

A plausible explanation of Fig. 1 is the different ionization mechanisms of EI and MPI. The cross section of electron impact ionization for helium at 300 eV is 28 Mb based on the database from National Institute of Standards and Technology.[24] Although there is no data for the cross section

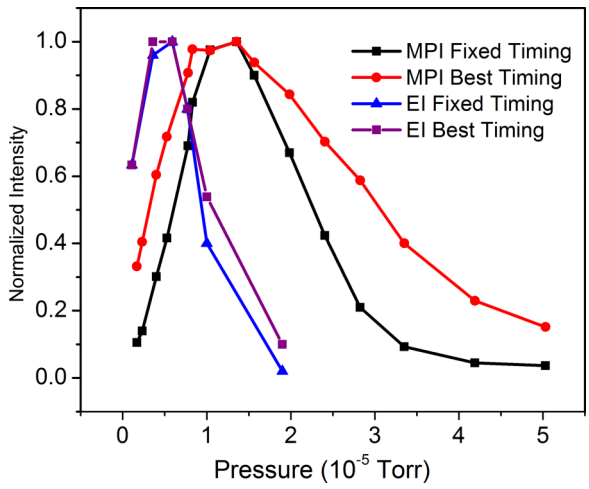

FIG. 1. Dependence of electron impact ionization and multiphoton ionization of CCl_4 doped helium droplets on the doping pressure recorded at a source temperature of 16 K and a stagnation pressure of 50 atm. The MPI trace labeled "fixed timing" was recorded at the optimal timing of the laser pulse obtained at a doping pressure of 1×10^{-5} Torr, while the EI trace labeled "fixed timing" was recorded at the timing determined at a doping pressure of 6×10^{-6} Torr. The profiles labeled "best timing" were obtained by adjusting the timing of the ionization pulse at each doping pressure.

of CCl_4, based on the values for CCl_nF where n = 1 to 3, an upper estimate of 1000 Mb can be assumed. Thus, it takes less than 40 helium atoms to shadow a CCl_4 molecule during EI. For a droplet containing over a thousand helium atoms and one CCl_4 molecule, the first ionized species should be helium atoms surrounding the dopant. The ionization yield should thus be reflective of the size of the droplet: assuming a constant probability of charge transfer, larger droplets are highly favored in producing dopant ions in EI.

For MPI, on the other hand, only doped CCl_4 can be ionized given the limited photon flux. Superfluid helium is transparent in the ultraviolet and based on the lack of any ion signal without dopant, we are confident that no substantial absorption is possible under our current laser intensity. Hence, absorption of CCl_4 at 266 nm is not affected by the surrounding helium atoms. It takes three photons to ionize one CCl_4 molecule and to produce one CCl_3^+ ion, and 5 photons are needed to produce Cl^+.[25] Power dependent studies of the yield of Cl^+ have revealed a second order relation—a significant but not full saturation.[20] With increasing doping pressure, more droplets are doped and more than one dopant molecule can reside in one droplet, and both result in increased yields of dopant fragments at high doping pressures.

Timing dependence

During the MPI experiment, we noticed that the best timing for the dopant fragments also changed with the doping pressure. Fig. 2 shows the time profile of Br^+ from MPI of doped CBr_4 at two different nozzle temperatures. Similar results were also obtained with CCl_4, but our data for CBr_4 are much more complete. The delay time in Fig. 2 is the time between the trigger signal to the pulsed valve and the onset of the laser pulse. In a previous publication,[20] we have established the existence of a primary and a rebound droplet pulse under our experimental conditions and have detailed the different pickup probabilities of the two pulses at different source temperatures. When the nozzle temperature is below 13 K, the rebound pulse contains enough large droplets for effective doping, so the earlier pulse at 8.5 K contains abundant dopant.[20] Since the rebound pulse has an effect of depleting the dopant concentration in the doping chamber, the amount of dopant in the primary pulse is smaller. Above 13 K, the rebound pulse does not contain sufficiently large droplets for effective doping and dopant depletion, hence the primary pulse contains more dopant molecules.

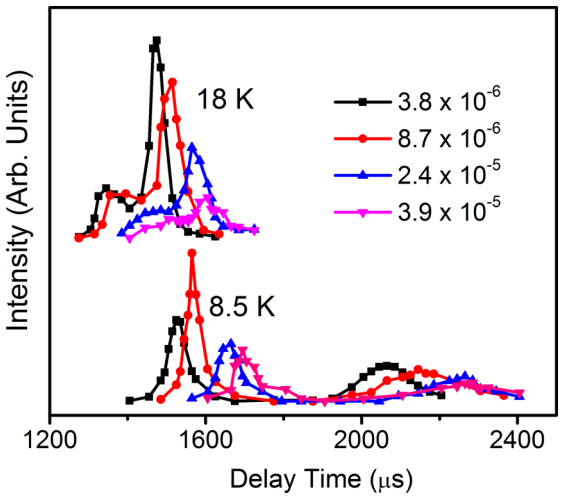

FIG. 2. Time profiles of Br^+ at different doping pressures of CBr_4 (in Torr) from the MPI-TOF recorded at source temperatures of 8.5 K and 18 K. The delay time refers to the time between the electrical trigger signal to the pulsed valve and the time of the laser pulse for ionization. Only one of the peaks at each temperature contains a substantial amount of dopant molecules.

The shift in timing with doping pressures at both source temperatures, up to 200 μs, is noticeable. The mechanism is related to the different speeds of different-sized clusters in a droplet beam, i.e., velocity slip.[26] The electrical pulse of the pulsed valve (24.8 μs) is much shorter than the flight time from the pulsed valve to the ionization region (>1 ms), hence all droplets can be regarded as formed at the same the time from the pulsed valve. The much longer duration of the actual droplet pulse probed in Fig. 2, more than 200 μs in time spread among the sampled doping pressures, should therefore be predominantly due to the different velocities of the different sized droplets. Smaller droplets have higher speeds and are at the front of the pulsed beam, and they are easily destroyed with doping. Larger slower droplets survive the doping process but they reach the detection region at a later time. This change in timing with doping pressure is particularly important for pulsed droplet beams, since the doping pressure directly affects the timing of the excitation beam.

This realization prompted us to revisit Fig. 1, for both the MPI and EI experiments. At each doping pressure, we varied the timing of the ionization pulse to find the best ion signal, and the resulting pressure profiles are designated as the "best timing" profiles. The MPI profile labeled "fixed timing" was obtained by optimizing the timing at a doping pressure of 1×10^{-5} Torr, hence at this pressure, the two MPI experiments have the same signal strength. At lower doping pressures, the "best timing" profile extends further into the region with lower doping pressures, while at higher doping pressures, the "best timing" profile extends to much higher pressures. At 3×10^{-5} Torr, the MPI signal shows a more than 3-fold increase under the "best timing" condition. In contrast, the EI signal shows limited improvement as the timing is varied at different doping pressures. In fact, the best timing for EI is within 50 μs of the original timing set at a doping pressure of 6×10^{-6} Torr. The effect of velocity slip in the EI experiment seems to be weaker than in the MPI experiment.

Analysis

A qualitative modeling of both the MPI and EI processes can be achieved based on Poisson pickup statistics.[27] We can calculate the probability of a droplet containing n helium atoms capturing k number of molecules $P_k(\rho; n)$ at a dopant gas density ρ. Unfortunately, the analytical expression from Poisson statistics[27] is based on negligible changes in the droplet size upon collisions. The most probable size of our droplet beam is ~2000 atoms/droplet[28] and pickup of one CCl_4 reduces the size by nearly 1/3. For these small-sized

droplets, size reduction has to be taken into consideration. For qualitative modeling, we modified the expression for the pickup probability by

$$P_k(\rho; n) = \frac{{z_k}^k}{k!} \exp(-z_k), \quad (1)$$

where z_k is the effective cross section for picking up k molecules with $z_1 = \rho \cdot \sigma_{e0} \cdot L$ and L (30 cm) is the length of the doping cell. The effective capture cross section σ_{e0} of an undoped droplet is considered proportional to the physical size of the droplet $\sigma_0 = \pi r_0^2$ with $r_0 = 2.22 \sqrt[3]{n}$ (Å). After picking up one dopant molecule, a droplet reduces its size by N_1 (500–700 helium atoms[29]) to $n_1 = n - N_1$, and the new pickup cross section is reduced to $\sigma_1 = \pi r_1^2$ with $r_1 = 2.22 \sqrt[3]{n_1}$ (Å), so the effective pickup cross section across the whole length of the doping cell is $\sigma_{e1} = (\sigma_0 + \sigma_1)/2$, and the corresponding $z_2 = \rho \cdot \sigma_{e1} \cdot L$. For a droplet containing only 2000 helium atoms, the maximum doping number is $k_{max} = 3$, with $\sigma_{e3} = (\sigma_0 + \sigma_1 + \sigma_2)/3$. In practice, however, a helium reserve is required to transport the doped droplet from the doping region to the detection region and to limit the gain in transverse velocity from side-on collisions with dopant molecules, hence the maximum doping number should be smaller than the thermal dynamic limit n/N_1.

Modeling the MPI pressure profiles

During the MPI experiment, the laser has a duration of 5 ns, hence ionization should only probe droplets of a fixed size, assuming sufficient velocity slip in the droplet beam. If the timing of the ionization laser is fixed, then the same-sized droplets are detected throughout the whole range of pressures for the profile labeled "fixed timing" in Fig. 1. The signal in the MPI experiment should depend on the number of dopant molecules in the droplet beam. Here we ignore the dependence of the ionization mechanism on cluster size,[30] and assume that the yield of Cl^+ ions $I_{MPI}(\rho; n)$ is proportional to the number of doped molecules k:

$$I_{MPI}(\rho; n) \propto \sum_{k=1}^{k_{max}} k \cdot P_k(\rho; n). \quad (2)$$

To compare with the experiment under "fixed timing," we varied n from 1000 to 10 000, k_{max} from 1 to n/N_1, and N_1 from 500–700,[29] and the calculated maximum intensity from each set of (n, k_{max}, N_1) as a function of doping pressure was normalized to a value of 1. We then calculated the square deviations of the intensities at different pressures between the calculation and experiment. The values of N_1 did not affect the general shape of the profile, hence it was set at 600. When the square deviations are plotted against values of n and k_{max}, a trough can be observed as shown in Fig. 3(a). In the range of n = 1000–6000, the trough can be roughly fit with an equation $k_{max} = (n - 600)/600$, as shown by the straight line in the figure. Hence we conclude that in our MPI experiment, a helium reserve of 600 atoms is required to carry the doped droplets into the MPI-TOF and that the uptake of one room temperature CCl_4 molecule requires 600 helium atoms. We can ignore the bend of Fig. 3(a) in the region with $n > 6000$ based on conditions of our droplet source

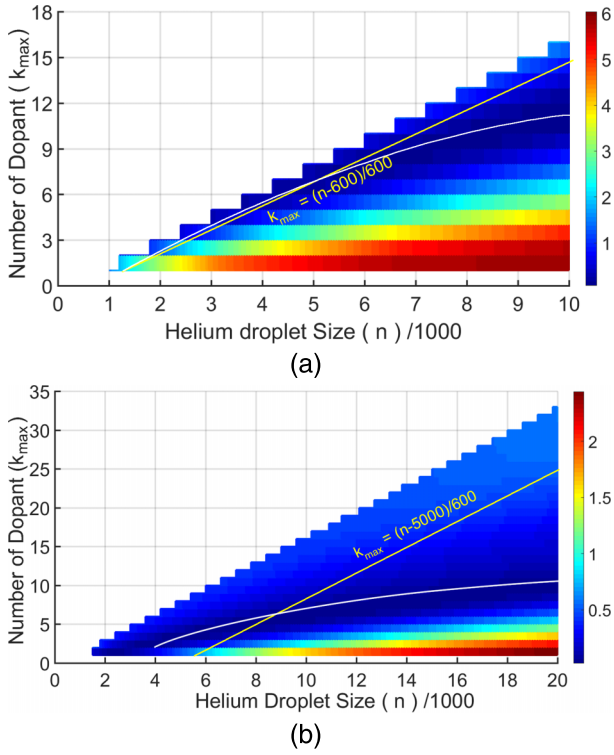

FIG. 3. Deviations of simulation results from experimental data plotted as functions of the droplet size n and the maximum number of dopant molecules k_{max} from experiments of: (a) MPI, and (b) EI under "fixed timing" conditions. The white continuous lines are just guides for the troughs in each panel.

(16 K at 50 atm), hence the general size range of our droplet beam.[28]

For the experiment under "best timing," at each doping pressure, the intensity from each sized droplet n was calculated according to Eq. (2), with the corresponding values of k_{max} chosen from the trough of Fig. 3(a). This intensity was then attenuated by the abundance of the corresponding droplet size in a log-normal distribution. The maximum intensity from the whole range of chosen n values was considered the intensity at the chosen doping pressure, and the corresponding n value was considered the sampled droplet size under the "best timing" conditions. The resulting pressure dependence was then normalized and compared with the experimental data. Square deviations of the pressure profiles under "best timing" conditions were obtained and minimized by varying the parameters of the log-normal size distribution. A log-normal size distribution function[31] is specified by two parameters, an average size and a standard deviation.[32] Our minimization process resulted in an optimal average size of 5000 with a standard deviation of 0.85. At a doping pressure of 1×10^{-5} Torr, the largest contribution to the ionization signal was from droplets containing 4700 helium atoms. Fig. 4 shows the calculated profiles overlaid with the experimental data for both timing scenarios, with n = 4700 and k_{max} = 6 for the profile under "fixed timing." Although the agreement is not quantitative, both calculations capture the essence of the experimental data.

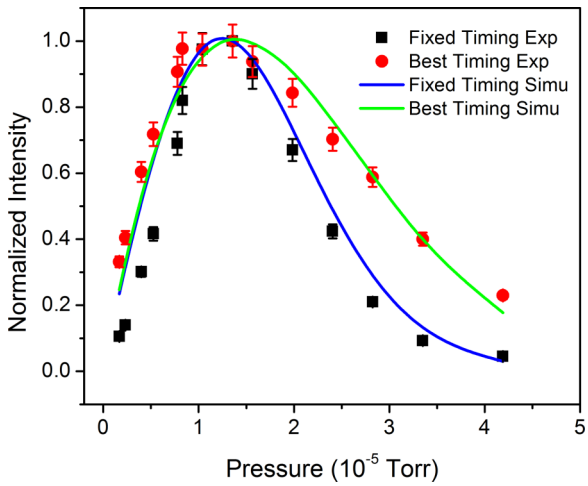

FIG. 4. Modeling of the MPI experiment using Eq. (2) under different timing conditions. The experimental data are reproduced from Fig. 1.

Modeling the EI pressure profiles

Electron impact ionization is dependent on the ionization of helium atoms, while ionization of dopant is a consequence of helium ionization. A different model is therefore required to simulate the EI profiles. The charge hopping model implies that regardless of the number of dopant molecules in a droplet, with the ionization of one helium atom, only one CCl_4 molecule can be ionized to produce one CCl_3^+. The overall ionization signal from the EI experiment is therefore proportional to the collective ionization cross section of the helium atoms in a droplet and the probability of picking up one or more dopant molecules,

$$I_{EI}(\rho; n) \propto \sum_{k=1}^{k_{max}} \sigma_{\mathrm{He}} \cdot (n - k \cdot N_1)^{2/3} \cdot P_k(\rho; n). \quad (3)$$

In Eq. (3), we have replaced the total ionization cross section of a droplet by $\sigma_{\mathrm{He}} \cdot n^{2/3}$, where σ_{He} is the ionization cross section of one helium atom.[15] Based on our numerical calculations, however, replacing the ionization cross section by $\sigma_{\mathrm{He}} \cdot n$ does not make any noticeable difference in the resulting pressure profiles. The mean free path of an electron with a kinetic energy of 300 eV in helium is ~30 Å based on the total collision cross section[33] and the density of superfluid helium,[32] hence for a droplet with less than 10^4 helium atoms and with a radius less than 100 Å, almost all helium atoms should have equal probability of being ionized in a droplet.

Equation (3) implies that the probability of charge transfer is constant throughout the size range of the probed droplets. This assumption is valid only when the dopant is located at the center of the droplet, and the size range of the sampled droplet, i.e., the square deviation of the log-normal distribution, is reasonably small. Ellis and Yang have modeled the probability of charge transfer by assuming a directed path of a helium cation to the dopant molecule for small sized droplets, and the result shows a more or less constant probability for droplets with average sizes above 2000.[33] The assumption of a directed path should break down for large sized droplets containing more than 50 000 atoms, and experimental results suggest much decreased probability than predicted by the model.[9,34] The calculation by Ellis and Yang was performed for electrons with a kinetic energy of 40 eV, while in our experiment, the impact energy was 300 eV, above the second ionization threshold of helium at 54 eV.[35] This difference can not only affect the total ionization cross section but also the mechanism of charge transfer. Given the complexity of the situation and the qualitative nature of our model, here we ignore the change in the probability of charge transfer with the droplet size, and consequently, we are cautious about any quantitative interpretation of our calculation result.

A few other considerations are included in the calculation of the EI profile. The EI experiment used an electric pulse of 4 μs in duration, much longer than the ionization laser pulse of 5 ns. However, considering the time scale of the velocity slip of several hundred microseconds, it is still reasonable to assume that the EI experiment only probes one sized droplets. The spectrometers for EI and MPI are at two different locations along the path of the droplet beam, and difference in timing between the two ionizing pulses can be calculated based on the average speed of the droplet beam. However, given the width of the EI pulse and the width of the laser pulse in the MPI experiment, this information is insufficient to determine if the EI pulse probes the same-sized droplets as the MPI pulse. To reach the EI-TOF after doping, a droplet has to travel an extra 12 cm to reach the ionizer and another 43 cm to reach the detector.[20] This situation requires a much larger droplet with a higher helium reserve than that of the MPI.

Similar to the approach used for the MPI calculation, to simulate the pressure profile of EI under "fixed timing," we normalized intensity distributions calculated from Eq. (3) for each n and k_{max} value while fixing N_1 at 600. The resulting pressure profile was compared with the experimental results obtained under "fixed timing," and the square deviations of the intensities are plotted in Fig. 3(b). The range of values for n was from 2000 to 20 000, and the range of values for k_{max} was the thermal dynamic limit n/N_1. Compared with the line represented by $k_{max} = (n - 5000)/600$, the trough in the plot of the square deviation has a much smaller slope, implying that more than 600 helium atoms are required to pick up one room temperature CCl_4 molecule and carry it to the EI-TOF.

To simulate the EI profile under the "best timing" conditions, we chose the same average size (5000 atoms/droplet) and standard deviation (0.85) as those from the calculation of the MPI profile to represent the log-normal distribution of the droplet beam. The ionization yield from Eq. (3) for each (n, k_{max}) pair in the trough of Fig. 3(b) was attenuated by the size distribution and then the highest ion yield was obtained at each doping pressure. The corresponding droplet size was then considered the sampled size in the "best timing" conditions. The resulting pressure profile was normalized and plotted on the same scale as that of the experimental data in Fig. 5. The calculation has no adjustable parameters, and the agreement is qualitatively satisfactory. At a doping pressure of 6×10^{-6} Torr, the maximum contribution to the ionization signal was from droplets containing 8300 helium atoms with $k_{max} = 5$, hence the corresponding pressure profile is plotted in Fig. 5 under "fixed timing" conditions. We therefore conclude that under the conditions of our EI-TOF, more than 5000 helium atoms are needed in a doped droplet for detection. While

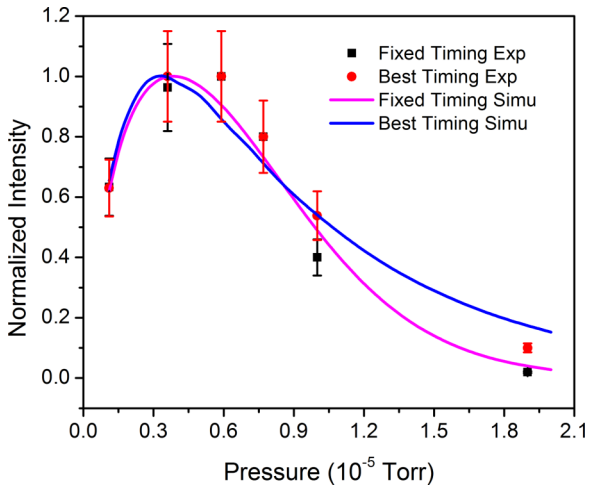

FIG. 5. Modeling of the EI experiment using Eq. (3) under different timing conditions. The experimental data are reproduced from Fig. 1.

this detection threshold seems large, it is a combination of several factors, including the ionization current of the electron beam, the detection efficiency of the mass spectrometer, and the probability of transport from the doping region to the detector.

Given the crudeness of the pickup model and the ionization models of Eqs. (2) and (3), the agreement of Figs. 4 and 5 is remarkable. Attempts to simply include an exponential decay function in Eq. (3) with a decay constant on the scale of the mean free path of an electron, similar to the method of Ref. 33, did not result in substantial improvement in the level of agreement. Further improvements in the calculation will perhaps require a numerical simulation of the pickup statistics, for which no closed-form analytical expression is possible.

The different behaviors of the MPI and EI experiments under "best timing" conditions can be understood from the following consideration. In the MPI experiment, every additional dopant molecule picked up by a droplet can potentially yield one extra Cl^+. Hence smaller droplets ($n = 4700$) and higher doping ($k_{max} = 6$) conditions are favored. The EI experiment is the contrary: once a single dopant molecule is picked up, additional doping is detrimental to the final ion yield. One reason is that doping decreases the ionization cross section by decreasing the droplet size through helium evaporation. Another reason is that the extra dopant molecule is not ionized to contribute to the observed ion signal since one helium ion can transfer its charge only to one neutral dopant molecule. On the other hand, a higher doping pressure also increases the fraction of doped droplets and hence increasing the ion yield. Consequently, a more delicate balance is required in the EI experiment, resulting in a narrower optimal pressure range for ion production. For a log-normal distribution with an average size of 5000 atoms/droplet and a standard deviation of 0.85, the most probable droplet size is 2000. While the optimal droplet size for the highest ionization yield of MPI is about the same as the average size, the corresponding value for EI is much larger, mostly because of the larger helium reserve (5000).

EI vs MPI: Relative yield

A comparison between the relative yields of MPI and EI is informative in understanding the current experimental results. There is no reported three photon absorption cross section for CCl_4 at 266 nm, but the one photon absorption cross section is on the order of 10^{-4} Mb.[36] For a single photon process at 266 nm, with a photon density of over 10^{28} photons/s cm^2, the probability of excitation in 5 ns is about 10^{-3}. A three photon process should have a comparable excitation probability since we are operating in a partial saturation scheme. In comparison, the effective ionization cross section of 8000 helium atoms is 2.2×10^5 Mb for collisions with electrons at 300 eV,[24] but the density of electrons is limited by the space charge effect to 10^7 cm^{-3}. If the interaction path length between the electrons and the droplets is on the order of 1 cm (the reality was more likely to be 0.5 cm), the probability of ionization is 10^{-6}, about 0.1% of that of MPI. In the calculations of Figs. 4 and 5, optimal EI requires a size of 8300, while optimal MPI requires a size of 4700. This condition further reduces the yield of EI by a factor of three because of the size distribution of the droplet beam. The deficiency in ionization from the EI experiment can be partially compensated for by the larger sampling fraction of doped droplets, because the ionization volume of EI encompasses the whole doped droplet beam, while only a small fraction of the beam is sampled in the MPI experiment. However, the collection efficiency of the EI-TOF is substantially lower than that of the MPI-TOF because of the longer path length and inefficient space focusing. An unknown factor is the yield of CCl_3^+ for each helium ion in a droplet and of Cl^+ after multiphoton ionization of one CCl_4. Assuming both unknowns are about the same order of magnitude, the overall signal for EI should be comparable to or weaker than that of MPI. Experimentally, we have observed three orders of magnitude deficiency in the signal strength of EI.

The above consideration did not include the caging effect of superfluid helium droplets in the MPI process. Less than unity escaping probability of photofragments in superfluid helium droplets has been documented in several previous works.[17,37] For example, Braun and Drabble have investigated photodissociation of CH_3I and its structural analogues at different dissociation wavelengths.[37] They have been able to reproduce the escaping probability using a classical binary collision model. The most probable droplet size in our experiment is ~2000 atoms/droplet, much smaller than those used in previous studies. The small mass of a helium atom is ineffective in slowing down a massive fragment like Cl^+.

A word of caution and a solution

Our results tell a cautionary tale in using mass spectrometry to characterize the doping conditions of a droplet beam. Depending on the nature of investigation, the best doping conditions and the best timing of a pulsed droplet beam vary. Electron impact ionization benefits from the collective large ionization cross sections of helium atoms in a droplet, but its sensitivity suffers under heavy doping conditions because of the loss of helium atoms. In this sense, EI is an ideal characterization method for experiments

that only concern with singly doped droplets, for example, spectroscopic investigations. The MPI experiment with a moderate laser power, on the other hand, is partially blind to the droplet condition and blind to the presence of dopant clusters, but it is sensitive to the presence of dopant molecules. Caution has to be exerted when using MPI to optimize the doping pressure for experiments of singly doped molecules.

By taking advantage of the velocity slip and the doping statistics, we can devise an approach to maximize the signal from singly doped droplets and to minimize the interference of dopant clusters. If the excitation is pulsed, we can first find the timing of the excitation pulse based on the diagnostic signal at a low doping pressure. This time setting eliminates contributions of larger-sized droplets and dopant clusters, regardless of doping conditions. Then we can increase the doping pressure and maximize the dopant related signal. Multiply-doped large droplets are too slow to be sampled by the pulsed excitation pulse, and small droplets that survive the doping region should be mostly singly doped. This scheme is more effective for larger dopants with higher heat capacities (larger N_1 value), because evaporative cooling generates a bigger size difference between singly doped and doubly doped droplets and hence a larger velocity slip. Using this scheme, we have obtained electron diffraction from a droplet beam with 95% of the droplets containing just one ferrocene molecule, and based on the analysis of the diffraction pattern, there is no contribution from ferrocene clusters.

CONCLUSION

We have compared the characteristics of electron impact ionization and non-resonant multiphoton ionization using the same droplet source. The first event in an EI experiment is ionization of helium atoms in pure or doped droplets, hence the signal of EI is reflective of droplet sizes. The limited photon density of a focused laser beam, on the other hand, has a higher probability of ionizing dopant molecules than helium atoms, hence MPI is only related to the average number of dopant molecules in a droplet. Using a crude model for the pickup statistics and simple models for EI and MPI, we have been able to simulate the pressure profiles of both the EI and MPI experiments performed under different conditions. This comparison offers a word of caution in using different ionization methods for characterization of superfluid helium droplets. Not only the doping pressure for optimal signal strength would be different for EI and MPI but also the exact timing of arrival of doped droplets in a pulsed droplet beam. On the other hand, this work also alludes to a scheme to reach a high fraction of doping while limiting the contribution of clusters.

ACKNOWLEDGMENTS

This work is supported by the National Institute of General Medical Sciences (No. 1R01GM101392-01A1) from the National Institutes of Health and the Environmental Health Science Center at Oregon State University funded by the National Institute of Environmental Health Sciences (No. ES000210).

[1]J. P. Toennies and A. F. Vilesov, Angew. Chem., Int. Ed. **43**, 2622 (2004).
[2]W. Kong, L. Pei, and J. Zhang, Int. Rev. Phys. Chem. **28**, 33 (2009).
[3]S. Yang and A. M. Ellis, Chem. Soc. Rev. **42**, 472 (2013).
[4]J. Zhang, L. Chen, W. M. Freund, and W. Kong, J. Chem. Phys. **143**, 074201 (2015).
[5]J. Zhang, Y. He, W. M. Freund, and W. Kong, J. Phys. Chem. Lett. **5**, 1801 (2014).
[6]J. C. H. Spence and R. B. Doak, Phys. Rev. Lett. **92**, 198102 (2004).
[7]M. Mudrich and F. Stienkemeier, Int. Rev. Phys. Chem. **33**, 301 (2014).
[8]H. Schöbel, P. Bartl, C. Leidlmair, S. Denifl, O. Echt, T. D. Märk, and P. Scheier, Eur. Phys. J. D **63**, 209 (2011).
[9]S. Yang, S. M. Brereton, M. D. Wheeler, and A. M. Ellis, J. Phys. Chem. A **110**, 1791 (2006).
[10]M. N. Slipchenko, S. Kuma, T. Momose, and A. F. Vilesov, Rev. Sci. Instrum. **73**, 3600 (2002).
[11]H. Buchenau, J. P. Toennies, and J. A. Northby, J. Chem. Phys. **95**, 8134 (1991).
[12]T. Ruchti, K. Forde, B. E. Callicoatt, H. Ludwigs, and K. C. Janda, J. Chem. Phys. **109**, 10679 (1998).
[13]H. Schöbel, M. Dampc, da. S. F. Ferreira, A. Mauracher, F. Zappa, S. Denifl, T. D. Märk, and P. Scheier, Int. J. Mass Spectrom. **280**, 26 (2009).
[14]A. Scheidemann, B. Schilling, and J. P. Toennies, J. Phys. Chem. **97**, 2128 (1993).
[15]B. E. Callicoatt, D. D. Mar, V. A. Apkarian, and K. C. Janda, J. Chem. Phys. **105**, 7872 (1996).
[16]D. S. Peterka, J. H. Kim, C. C. Wang, L. Poisson, and D. M. Neumark, J. Phys. Chem. A **111**, 7449 (2007).
[17]D. S. Peterka, J. H. Kim, C. C. Wang, and D. M. Neumark, J. Phys. Chem. B **110**, 19945 (2006).
[18]S. A. Krasnokutski and F. Huisken, J. Chem. Phys. **142**, 084311 (2015).
[19]X. Zhang and M. Drabbels, J. Phys. Chem. Lett. **5**, 3100 (2014).
[20]Y. He, J. Zhang, Y. Li, W. M. Freund, and W. Kong, Rev. Sci. Instrum. **86**, 084102 (2015).
[21]Y. Ovcharenko, V. Lyamayev, R. Katzy, M. Devetta, A. La Forge, P. O'Keeffe, O. Plekan, P. Finetti, M. Di Fraia, M. Mudrich, M. Krikunova, P. Piseri, M. Coreno, N. B. Brauer, T. Mazza, S. Stranges, C. Grazioli, R. Richter, K. C. Prince, M. Drabbels, C. Callegari, F. Stienkemeier, and T. Moeller, Phys. Rev. Lett. **112**, 073401 (2014).
[22]Y. J. Kime, D. C. Driscoll, and P. A. Dowben, J. Chem. Soc., Faraday Trans. **2**(83), 403 (1987).
[23]Y.-L. He and L. Wang, Struct. Chem. **20**, 461 (2009).
[24]*Electron-Impact Cross Sections for Ionization and Excitation*, edited by Y.-K. Kim, K. K. Irikura, M. E. Rudd, M. A. Ali, P. M. Stone, J. Chang, J. S. Coursey, R. A. Dragoset, A. R. Kishore, K. J. Olsen, A. M. Sansonetti, G. G. Wiersma, D. S. Zucker, and M. A. Zucker (National Institute of Standards and Technology, Gaithersburg, MD, 2011).
[25]G. R. Burton, W. F. Chan, G. Cooper, and C. E. Brion, Chem. Phys. **181**, 147 (1994).
[26]S. Yang and A. M. Ellis, Rev. Sci. Instrum. **79**, 016106 (2008).
[27]M. Hartmann, R. E. Miller, J. P. Toennies, and A. F. Vilesov, Science **272**, 1631 (1996).
[28]L. F. Gomez, E. Loginov, R. Sliter, and A. F. Vilesov, J. Chem. Phys. **135**, 154201 (2011).
[29]M. Lewerenz, B. Schilling, and J. P. Toennies, J. Chem. Phys. **102**, 8191 (1995).
[30]L. S. Cederbaum, J. Zobeley, and F. Tarantelli, Phys. Rev. Lett. **79**, 4778 (1997).
[31]M. Lewerenz, B. Schilling, and J. P. Toennies, Chem. Phys. Lett. **206**, 381 (1993).
[32]J. Harms, J. P. Toennies, and F. Dalfovo, Phys. Rev. B **58**, 3341 (1998).
[33]A. M. Ellis and S. Yang, Phys. Rev. A: At., Mol., Opt. Phys. **76**, 032714 (2007).
[34]W. K. Lewis, B. E. Applegate, J. Sztaray, B. Sztaray, T. Baer, R. J. Bemish, and R. E. Miller, J. Am. Chem. Soc. **126**, 11283 (2004).
[35]Z. Zhang, L.-Y. Peng, M.-H. Xu, A. F. Starace, T. Morishita, and Q. Gong, Phys. Rev. A: At., Mol., Opt. Phys. **84**, 043409 (2011).
[36]C. Hubrich and F. Stuhl, J. Photochem. **12**, 93 (1980).
[37]A. Braun and M. Drabbels, J. Chem. Phys. **127**, 114303 (2007).